Journal of Alloys and Compounds 526 (2012) 79–84

Contents lists available at SciVerse ScienceDirect

Journal of Alloys and Compounds

journal homepage: www.elsevier.com/locate/jallcom

Piezoelectric and ferroelectric properties of $(Bi_{1-x}Na_{0.8}K_{0.2}La_x)_{0.5}TiO_3$ lead-free ceramics

Baoyin Wang, Laihui Luo*, Feng Ni, Peng Du, Weiping Li, Hongbing Chen

Department of Physics, Ningbo University, Ningbo 315211, China

ARTICLE INFO

Article history:
Received 15 January 2012
Received in revised form 14 February 2012
Accepted 18 February 2012
Available online xxx

Keywords:
Lead-free ceramic
Piezoelectric
Dielectric
Depolarization
Strain

ABSTRACT

Lead-free piezoelectric ceramics $(Bi_{1-x}Na_{0.8}K_{0.2}La_x)_{0.5}TiO_3$ were synthesized successfully by conventional solid state reaction method. The piezoelectric, dielectric and ferroelectric characteristics of the ceramics were investigated and discussed. The XRD results show that La^{3+} has diffused into $(BiNa_{0.8}K_{0.2})_{0.5}TiO_3$ (BNKT) lattices to form a new solid solution $(Bi_{1-x}Na_{0.8}K_{0.2}La_x)_{0.5}TiO_3$ with a pure perovskite structure. Partial substitution of La^{3+} for Bi^{3+} in the BNKT ceramics can enhance their piezoelectric, without an obvious decline of ferroelectric properties. The piezoelectric measurements and *P–E* hysteresis loops reveal that the ceramic with $x = 0.005$ has the highest piezoelectric performance and strong ferroelectricity. At high La^{3+} level ($x > 0.04$), the low dielectric anomaly at T_d disappears. A maximum strain of 0.16% is obtained at $x = 0.02$ for the $(Bi_{1-x}Na_{0.8}K_{0.2}La_x)_{0.5}TiO_3$ ceramic. The depolarization temperature T_d decreases with x increasing ($x = 0$–0.08), and the depolarization mechanism is analyzed.

1. Introduction

Lead-based piezoelectric Pb(Zr, Ti)O_3 (PZT) ceramics with high piezoelectric constant response near morphotropic phase boundary (MPB) are widely used in actuators, transducers and other electromechanical devices [1]. However, the use of PZT piezoelectric ceramics has caused serious lead pollution and environmental problems because of the high toxicity of lead oxide and its high volatility during sintering. Therefore, the development of lead-free piezoelectric ceramics with satisfactory piezoelectric properties attracts much attention [2]. Among lead-free piezoelectric ceramic materials, $Bi_{0.5}Na_{0.5}TiO_3$ (BNT) is considered to be a promising candidate for lead-free piezoelectric ceramics for its large remnant polarization ($P_r = 38\ \mu C/cm^2$) and high Curie temperature ($T_c = 320\ ^\circ C$). However, Compared with PZT ceramic, a pure BNT ceramic has poor piezoelectric properties ($d_{33} = 58$ pC/N) due to a high coercive field ($E_c = 7.3$ kV/mm) [3,4]. In order to improve the piezoelectric properties, lots of other perovskite ferroelectrics are added into BNT to form new BNT-based solid solutions, such as BNT–$BaTiO_3$ [BNT–BT] [5–7], BNT–$Bi_{0.5}K_{0.5}TiO_3$ [BNT–BKT] [8,9], BNT–$BaTiO_3$–$Bi_{0.5}Li_{0.5}TiO_3$ [10], $(Bi_{0.5}Na_{0.5})Ti_{1-x}(Zn_{1/3}Nb_{2/3})_xO_3$ [11], BNT–Ba(Ti, Zr)O_3 [12], BNT–BT–$La_{0.5}Na_{0.5}TiO_3$ [13]. Among these BNT-based ceramics, the BNT–BT and BNT–BKT ceramics have been studied most intensively because of their relatively high piezoelectric performances and simple compositions [2–6].

In PZT ceramic, low symmetry phases such as monoclinic and orthorhombic phases exist near MPB, which bridge rhombohedra-tetragonal phase transition. It is known that BNT-based ceramics have more complex phase structure near MPB. On one hand, from the above mentioned BNT-based systems, the partial substitutions of Bi^{3+} and Na^+ by other ions such as Ba^{2+}, K^+ and Li^+ in the BNT lattice have been extensively investigated. However, there is little report on the partial substitution of Bi^{3+} by other trivalent cations in the BNT ceramics. To obtain excellent electrical and optical properties of the ceramics, La is often used in PZT as an additive. On the other hand, $0.8Bi_{0.5}Na_{0.5}TiO_3$–$0.2Bi_{0.5}K_{0.5}TiO_3$ ($(BiNa_{0.8}K_{0.2})_{0.5}TiO_3$, BNKT) locates at MPB, and it has a relatively high piezoelectric response. Therefore, $(Bi_{1-x}Na_{0.8}K_{0.2}La_x)_{0.5}TiO_3$ is chosen as a basic chemical formula in this study.

In this paper, a new BNT-based solid solution, $(Bi_{1-x}Na_{0.8}K_{0.2}La_x)_{0.5}TiO_3$, was developed by the partial substitution of La^{3+} for Bi^{3+} in the $(Bi_{1-x}Na_{0.8}K_{0.2}La_x)_{0.5}TiO_3$ ceramics. The ceramics were prepared by a conventional ceramic method. The ferroelectric properties, piezoelectric performances, depolarization mechanism and field-induced strain of the ceramics were investigated and discussed.

2. Experiments

$(Bi_{1-x}Na_{0.8}K_{0.2}La_x)_{0.5}TiO_3$ ($x = 0$, 0.005, 0.01, 0.02, 0.04, 0.08) lead-free ceramics were prepared by a conventional solid state reaction technique. Analytical-grade powders: Bi_2O_3 (99.9%), Na_2CO_3 (99.8%), K_2CO_3 (99%), TiO_2 (99%) and La_2O_3 (99.95%) powders were used as starting materials. The powders in the stoichiometric ratio were mixed in alcohol by agate balls for 10 h, and then dried and calcined at 850 °C for 2 h. The calcined powders were reground by ball milling for 10 h. After drying, the powders were sieved and mixed thoroughly with a PVA binder solution, and then

* Corresponding author. Tel.: +86 574 87600953; fax: +86 574 87600744.
E-mail address: luolaihui@nbu.edu.cn (L. Luo).

0925-8388/$ – see front matter © 2012 Elsevier B.V. All rights reserved.
doi:10.1016/j.jallcom.2012.02.114

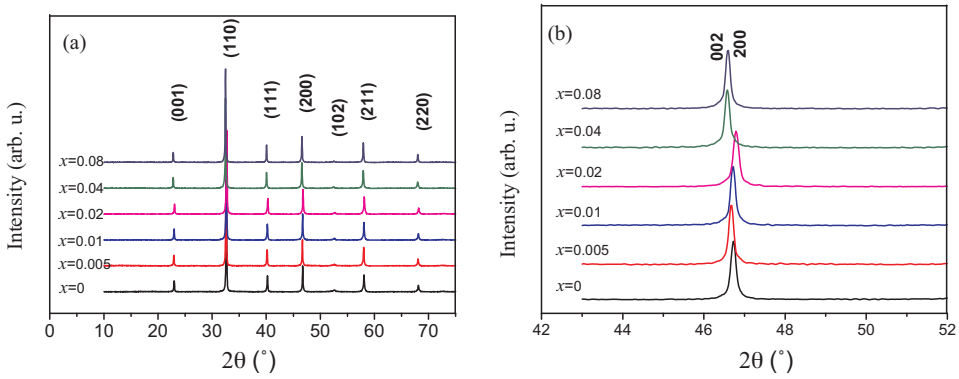

Fig. 1. XRD patterns of $(Bi_{1-x}Na_{0.8}K_{0.2}La_x)_{0.5}TiO_3$ ceramics.

uniaxially pressed into disk samples with a pressure of ~100 MPa. The disk samples were finally sintered at 1150 °C for 2 h in air. Silver paste was pasted on both sides of the disc samples and then fired at 600 °C in order to form electrodes. The samples were poled under a DC field of 4–5 kV/mm at 80 °C in silicone oil bath for 20 min, and then cooled to room temperature under the poling field.

The crystal structure of the ceramics was checked using X-ray diffraction (XRD) analyzer (Bruker D8 Advance) with Cu Kα radiation. The piezoelectric coefficient d_{33} of the samples was measured by a quasistatic piezoelectric meter (ZJ-3AN, China). Dielectric constant ε_{33} and dielectric loss tan δ of the sintered samples as a function of temperature at 10 kHz, 100 kHz and 1 MHz were measured using a computer-controlled impedance analyzer (Agilent 4294A). The polarization vs. electric field (P–E) hysteresis loops were obtained at 1 Hz by the RT Premier II ferroelectric workstation. The mechanical quality factor Q_m and electromechanical coupling factors k_p, k_t were calculated using the resonance–antiresonance method with the impedance analyzer. The field-induced strain of the specimens was measured using a laser interferometry with a frequency of 10 Hz.

3. Results and discussions

The XRD patterns of the $(Bi_{1-x}Na_{0.8}K_{0.2}La_x)_{0.5}TiO_3$ ceramics with $0 \le x \le 0.08$ are shown in Fig. 1(a). The diffraction patterns from Cu $K\alpha_2$ were removed by XRD analysis software JADE. The results suggest that all the ceramics possess a pure perovskite phase and no secondary impurity phase can be observed, indicating that La^{3+} has diffused into BNKT lattices to form a new solid solution $(Bi_{1-x}Na_{0.8}K_{0.2}La_x)_{0.5}TiO_3$. BNT is considered as a rhombohedral phase following the investigation of Jones and Thomas [14–16]. It is also reported that BNT is a monoclinic phase at room temperature [17,18]. Usually, BKT is regarded as tetragonal phase at ambient temperature. So when it comes to BNT's solid solution with BKT, the symmetry of the solid solution becomes more complex. It is reported that a sufficient amount of electric field can induce a tetragonal phase transition in the pseudocubic BNT-ceramics [19,20]. At room temperature, BNKT resides at the rhombohedral–tetragonal MPB [21–23], and the symmetry of $(Bi_{1-x}Na_{0.8}K_{0.2}La_x)_{0.5}TiO_3$ can be seen as pseudocubic structure within the resolution of XRD. The XRD patterns of samples in the 2θ ranging from 43° to 52° are zoomed in Fig. 1(b). As shown in Fig. 1(b), there is no splitting of the (2 0 0) peak, indicating that addition of La does not lead to a phase transition from the pseudocubic to a tetragonal phase. Partial substitution of La^{3+} into $(Bi_{1-x}Na_{0.8}K_{0.2}La_x)_{0.5}TiO_3$, leads to little change of the position of the (2 0 0) peak when x remains less than 0.02. The (2 0 0) Bragg peak shifts to a higher angle when $x = 0.02$, indicating contraction of the lattice. However, the same peak shifts to a lower angle when $x > 0.02$, suggesting an expansion of the lattice. Considering that the radii of La^{3+}, Bi^{3+} and Na^+ are 1.06, 1.03, and 1.02 Å, respectively, this behavior indicates that initially La^{3+} substitutes for Na^+ that leads to creation of oxygen vacancies and lattice contraction, but when x exceeds 0.02, La^{3+} begins to substitute for Bi^{3+}, thus leading to lattice expansion.

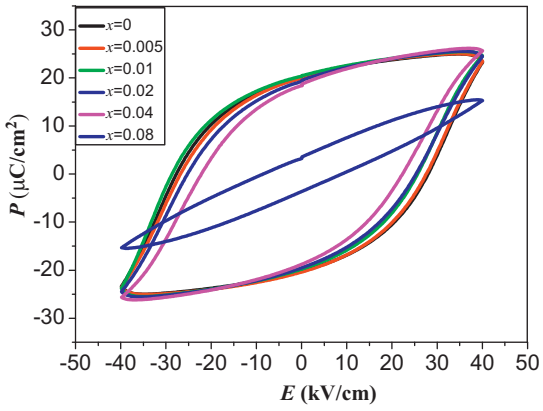

Fig. 2. P–E hysteresis loops of $(Bi_{1-x}Na_{0.8}K_{0.2}La_x)_{0.5}TiO_3$ at room temperature.

Fig. 2 shows the P–E hysteresis loops of the $(Bi_{1-x}Na_{0.8}K_{0.2}La_x)_{0.5}TiO_3$ ($x = 0$, 0.005, 0.01, 0.02, 0.04, 0.08) ceramics at room temperature. As illustrated in Fig. 2, all the $(Bi_{1-x}Na_{0.8}K_{0.2}La_x)_{0.5}TiO_3$ ceramics exhibit a character of typical ferroelectric hysteresis loop except $x = 0.08$. With x increasing to 0.04, the P–E loop varies little with x. When $x = 0.005$, the ceramic exhibits a strong ferroelectric property, giving an E_c of 27.2 kV/cm and P_r of 20.2 μC/cm^2. However, for $x = 0.08$, the P–E loop becomes flattened and slanted, indicating that the addition of the excess of La^{3+} weaken the ferroelectricity of the ceramics greatly. Fig. 3 presents the variations of the remnant polarization P_r and coercive field E_c with x. We can find that the P_r has no obvious change with x increasing and then decreases sharply at a high La^{3+} level. When $x = 0.08$, P_r reaches a low value of only 3.6 μC/cm^2. Effective E_c

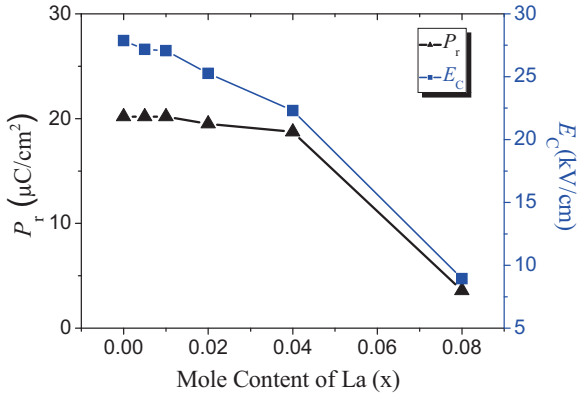

Fig. 3. Variations of P_r and E_c with x for the $(Bi_{1-x}Na_{0.8}K_{0.2}La_x)_{0.5}TiO_3$ ceramics.

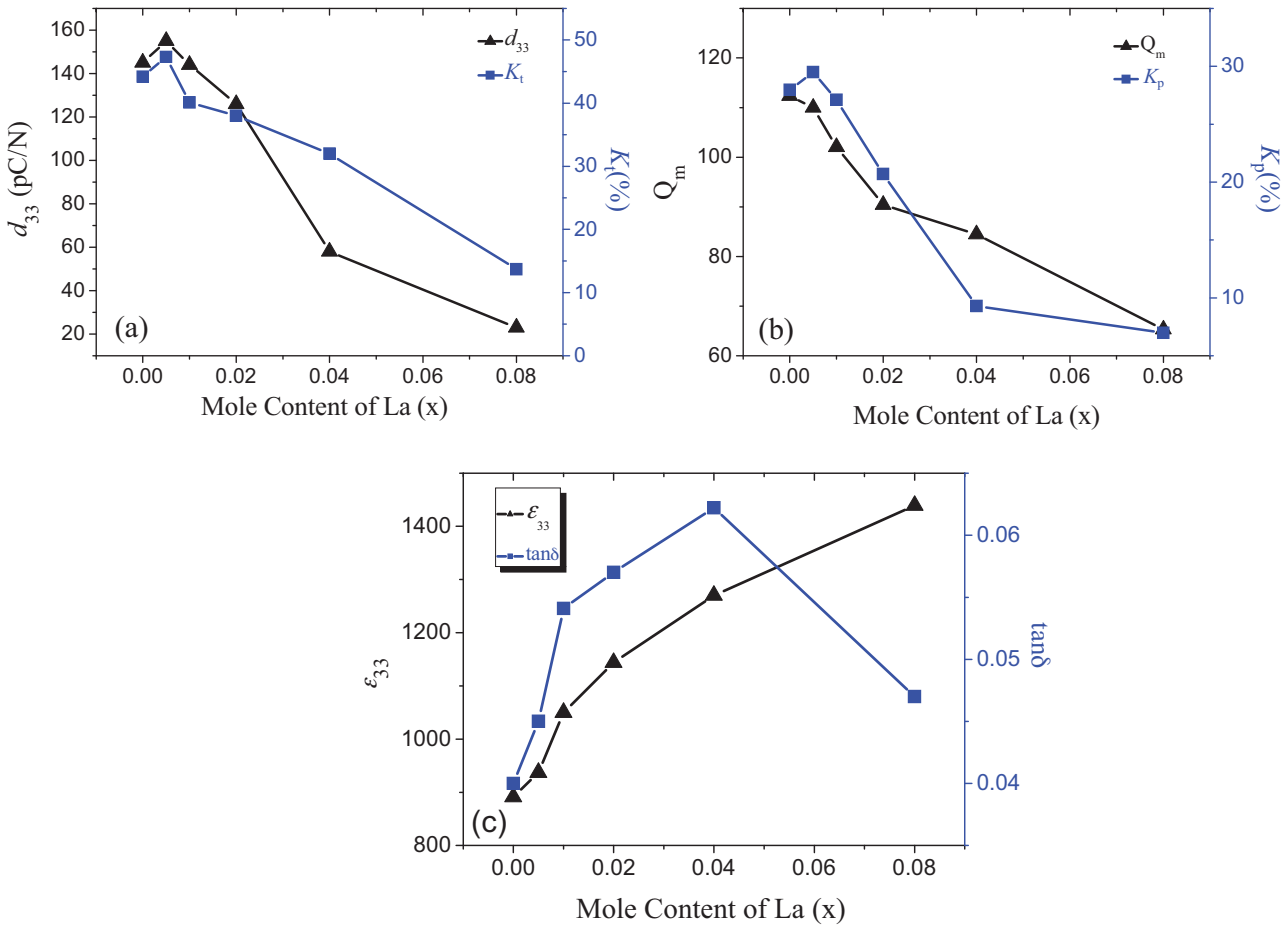

Fig. 4. (a) d_{33} and k_t of the $(Bi_{1-x}Na_{0.8}K_{0.2}La_x)_{0.5}TiO_3$ ceramics, (b) Q_m and k_p of the $(Bi_{1-x}Na_{0.8}K_{0.2}La_x)_{0.5}TiO_3$ ceramics, and (c) ε_{33} and tan δ of the $(Bi_{1-x}Na_{0.8}K_{0.2}La_x)_{0.5}TiO_3$ ceramics.

decreases steeply from 27.2 kV/cm to 8.9 kV/cm as x increases from 0 to 0.08. Obviously, the introduction of a small amount of La^{3+} into $(Bi_{1-x}Na_{0.8}K_{0.2}La_x)_{0.5}TiO_3$ ceramics lowers E_c and P_r slightly. However, after excessive content of La^{3+}, the ceramics exhibit very weak ferroelectricity. The weakness of the ferroelectricity of the ceramics at a high La^{3+} level ($x > 0.04$) should be attributed to the weakened ferroelectric phase induced by the substitution of La^{3+} in the $(Bi_{1-x}Na_{0.8}K_{0.2}La_x)_{0.5}TiO_3$ ceramics [24]. This is caused by the substitution of La^{3+} for Bi^{3+}, which brings about a decrease in deviated distance of B-site and O-site by moving atoms to body-centered and face-centered locations, respectively, thus making spontaneous polarization to decline. Such a weakness of the ferroelectricity can be also caused by the enhanced cation disorder by substitution of La^{3+} for Bi^{3+} at the A sites of the lattice.

Fig. 4(a) shows the variations of the piezoelectric coefficient d_{33}, electromechanically coupling factor k_t with x for $(Bi_{1-x}Na_{0.8}K_{0.2}La_x)_{0.5}TiO_3$ ceramics. It can be seen that after the substitution of La^{3+} for Bi^{3+}, the behaviors of d_{33}, k_t as a function of x are similar to each other. The d_{33} and k_t increase with x when $x < 0.005$, then decrease with x increasing further. At $x = 0.005$, maximum values of d_{33} and k_t are 155 pC/N and 47.3%, respectively. The enhancement of piezoelectricity of the $(Bi_{1-x}Na_{0.8}K_{0.2}La_x)_{0.5}TiO_3$ ceramics at $x = 0.005$ should be attributed to the easier domain movements and phase transition between rhombohedral and tetragonal phase [25]. However, $(Bi_{1-x}Na_{0.8}K_{0.2}La_x)_{0.5}TiO_3$ with $x = 0.08$ exhibit a much lower d_{33} of 23 pC/N and k_t of 13.7%. Fig. 4(b) presents the variations of Q_m and k_p of the $(Bi_{1-x}Na_{0.8}K_{0.2}La_x)_{0.5}TiO_3$ ceramics with x. As shown in Fig. 4(b), the behavior of k_p is similar to those of d_{33} and k_t as a function of x. At $x = 0.005$ and 0.08, maximum and minimum values of $k_p = 28\%$ and 7% are obtained, respectively. The Q_m for planar vibration mode decreases from 112.4 to 65.3 as x increases from 0 to 0.08. The decrement of Q_m is caused by the easier movement of domains, which will lead to a mechanical energy loss. The dielectric constant ε_{33} and dielectric loss tan δ, measured at 1 kHz, of $(Bi_{1-x}Na_{0.8}K_{0.2}La_x)_{0.5}TiO_3$ ceramics are shown in Fig. 4(c). The maximum values of $\varepsilon_{33} = 1439$ and tan $\delta = 0.062$ are obtained at $x = 0.08$ and 0.04, respectively.

Fig. 5 shows the temperature dependences of dielectric constant ε_{33} and dielectric loss tan δ for the $(Bi_{1-x}Na_{0.8}K_{0.2}La_x)_{0.5}TiO_3$ ceramics with $x = 0$, 0.005, 0.01, 0.02, 0.04 and 0.08 at 10 kHz, 100 kHz and 1 MHz. Fig. 5(a)–(e) shows that the ceramics with different La content exhibit three dielectric anomalies at T_d, T_p and T_m, as marked in the figures. The first one occurs at the depolarization temperature T_d. From Fig. 5(a)–(e), it can be seen that T_d is independent on the measurement frequency. T_d is not observed in Fig. 5(f), implying that T_d has moved to lower temperature than the measurement temperature. The second one appears at temperature T_p. Some researchers consider that phase transition from rhombohedral phase to tetragonal phase occurs at temperature T_p [26,27]. From Fig. 5(a)–(f), it can be known that T_p is dependent on the measurement frequency, suggesting that the dielectric anomaly is not caused by a phase transition. This dielectric anomaly might originate from the polarization of space charges and dipolar defects [28]. The third dielectric anomaly appears at temperature T_m, and T_m is the maximum temperature at which ε_{33} reaches a maximum value and corresponds to a transition from a non-polar state to a paraelectric state [29]. As shown in Fig. 5, the dielectric anomaly

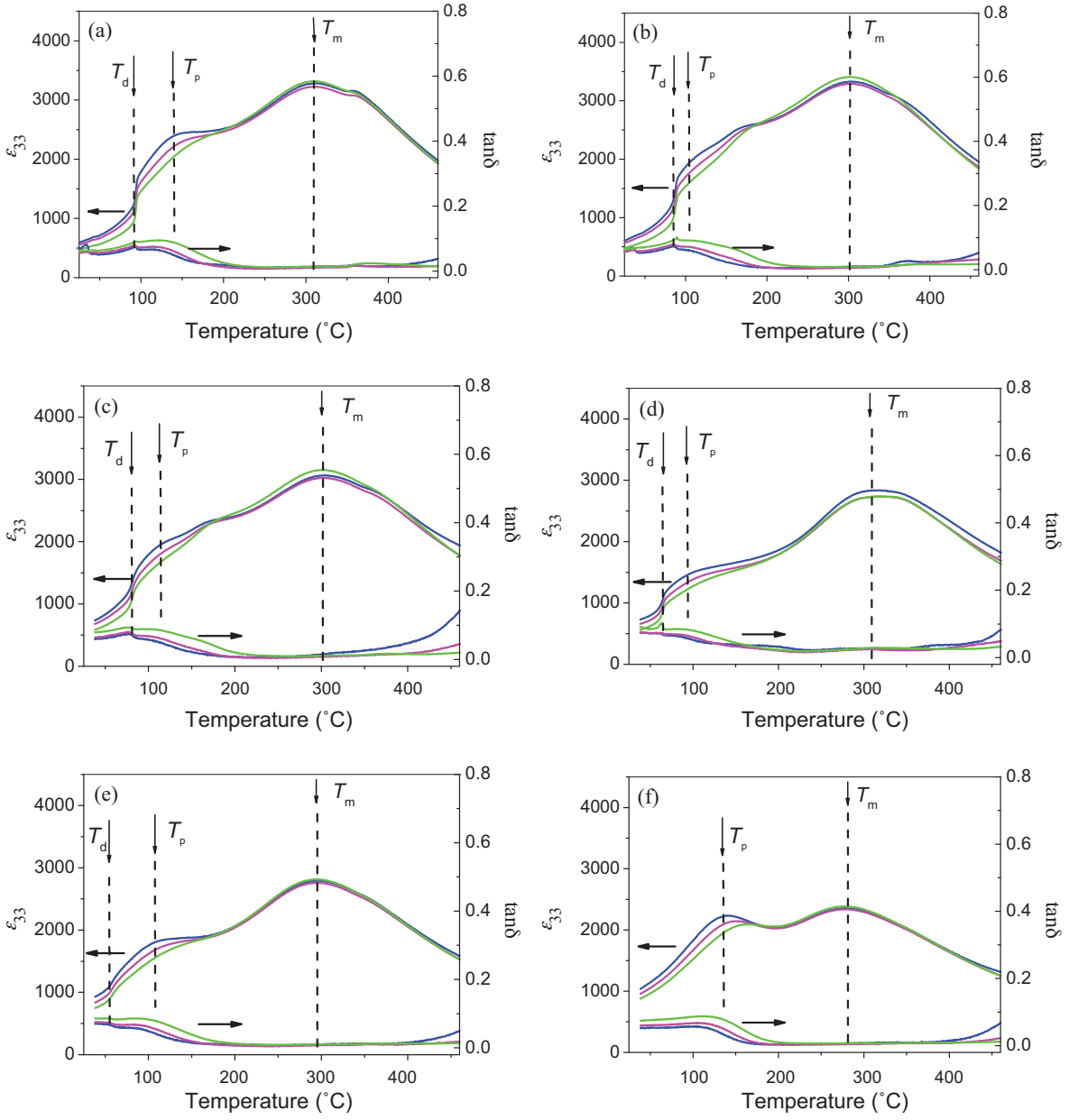

Fig. 5. Temperature dependences of ε_{33} and tan δ for poled $(Bi_{1-x}Na_{0.8}K_{0.2}La_x)_{0.5}TiO_3$ ceramics at 10 kHz, 100 kHz and 1 MHz: (a) $x = 0$, (b) $x = 0.005$, (c) $x = 0.01$, (d) $x = 0.02$, (e) $x = 0.04$, and (f) $x = 0.08$.

peaks at T_m for all the ceramics are relatively broad, indicating that the phase transition at T_m is a diffuse phase transition. Diffuse phase transition has always been observed in BNT-based ceramics [30,31], of which either the A-sites or B-sites are occupied by at least two cations. Na^+, K^+, Bi^{3+} and La^{3+} are randomly distributed in A-sites for $(Bi_{1-x}Na_{0.8}K_{0.2}La_x)_{0.5}TiO_3$ ceramics, so the observed diffuse phase transition behavior near T_m is reasonably attributed to the disordering of A-site cations.

T_d and T_m as a function of x for the $(Bi_{1-x}Na_{0.8}K_{0.2}La_x)_{0.5}TiO_3$ ceramics are shown in Fig. 6. T_d is corresponding to the temperature at the first tan δ peak [32]. With the La content increasing from 0 to 0.04, it can be seen that T_d decreases from 92 °C to 56 °C. When x increases to 0.08, T_d is not observed in the curve for ε_{33} and tan δ vs. temperature. Because of the lower T_d than ambient temperature, $(Bi_{1-x}Na_{0.8}K_{0.2}La_x)_{0.5}TiO_3$ ($x = 0.08$) exhibits weak ferroelectric properties and low piezoelectric coefficients at ambient temperature, as shown in Figs. 2 and 4, respectively.

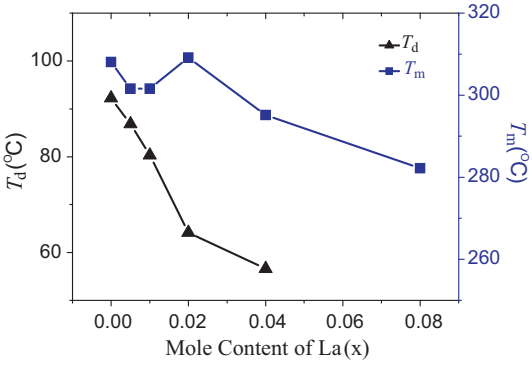

Fig. 6. T_d and T_m as a function of x for the $(Bi_{1-x}Na_{0.8}K_{0.2}La_x)_{0.5}TiO_3$ ceramics.

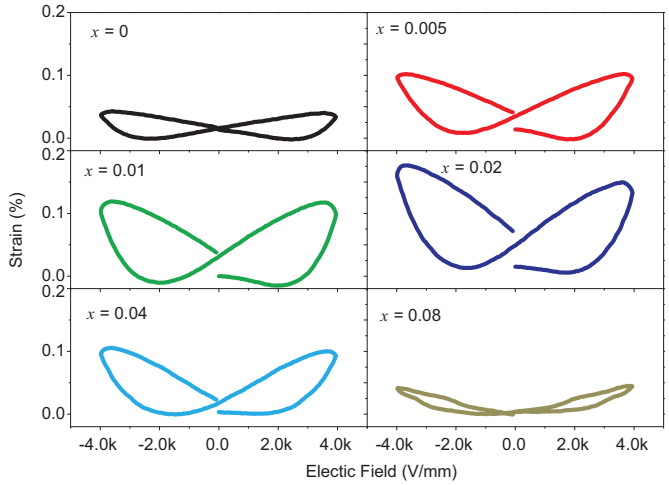

Fig. 7. Electric-field-induced strain for the $(Bi_{1-x}Na_{0.8}K_{0.2}La_x)_{0.5}TiO_3$ ceramics.

However, T_m of $(Bi_{1-x}Na_{0.8}K_{0.2}La_x)_{0.5}TiO_3$ ceramics varies little with x increasing.

Bipolar electric-field-induced strain of the ceramics is shown in Fig. 7. All the ceramics show a butterfly-shaped curve. From Fig. 7, we know that the ceramics with $x \leq 0.04$ shows a typical butterfly-shaped curve of ferroelectrics. The hysteresis, which is caused by the domain switching and phase transition induced by the electric field, is very large. The bipolar maximum strain of $(Bi_{1-x}Na_{0.8}K_{0.2}La_x)_{0.5}TiO_3$ ceramic is 0.16%, which is obtained at $x = 0.02$. However, the largest d_{33} is obtained at $x = 0.005$, as shown in Fig. 4(a). Generally speaking, large electric-field-induced strain means a large piezoelectric response. The results for electric-field-induced strain are not consistent with the piezoelectric coefficient d_{33} measured by quasistatic method. Lattice distortion and domain switching, which can be induced by electric field, contribute to the measured strain. Meanwhile, only lattice distortion contributes to d_{33} when measured by quasistatic method. The E_c and T_d of the ceramics decrease with the increment of La content x, as a result, the domain switches more easily. The joint action of lattice distortion and domain switching results in a largest stain is obtained in $(Bi_{1-x}Na_{0.8}K_{0.2}La_x)_{0.5}TiO_3$ ceramic when $x = 0.02$.

To obtain more details on the ferroelectric properties and depolarization mechanism of the ceramics, P–E hysteresis loops of $(Bi_{1-x}Na_{0.8}K_{0.2}La_x)_{0.5}TiO_3$ ($x = 0$, 0.005, 0.04) ceramics at different temperature have been measured under an electric field of 4 kV/mm, as shown in Fig. 8. All the ceramics exhibit a typical ferroelectric P–E loop at room temperature. From Fig. 8(a), it can be observed that the loop of $(Bi_{1-x}Na_{0.8}K_{0.2}La_x)_{0.5}TiO_3$ ceramic deforms and begins to form a constricted P–E hysteresis loop at 90 °C. At 100 °C, obvious double-like P–E hysteresis loop has formed and Pr is near zero, which is considered as a typical characteristic of anti-ferroelectrics. As determined from Fig. 8(a), the depolarization temperature T_d of the $(Bi_{1-x}Na_{0.8}K_{0.2}La_x)_{0.5}TiO_3$ ceramics with $x = 0$ is in the range of 90–100 °C, which is close to the value determined from tan δ peak (92 °C) (Fig. 5(a)). The ceramics with $x = 0.005$ and 0.04 exhibit similar temperature dependences of the P–E loops to the ceramic with $x = 0$, as shown in Fig. 8(b) and (c), respectively. Similar behavior of P–E hysteresis loops at different temperature is often observed in BNT-based ceramics [5,33–35]. Constricted or double-like P–E loops have been observed in BNT-based ceramics at high temperatures [36,37]. What causes a constricted hysteresis loop near T_d in the BNT-based materials? The researchers have different opinions on the depolarization mechanism. Some researchers roughly propose that the anomalies in the P–E loop resulted from the electromechanical interaction between the polar and the non-polar regions, which coexist in the ceramics at above T_d [24,36,37]. Some researchers consider that macro-micro domain transition occurs near T_d in BNT-based ceramics [30,31]. Most of the researchers consider that the appearance of the constricted hysteresis loop near T_d stems from phase transition from a ferroelectric phase to an anti-ferroelectric phase [33–35,38–41], which results in a large electric-field-induced strain. Constricted hysteresis loop and large electric-field-induced strain are considered as concrete proof of ferroelectric-antiferroelectric transition. However, double hysteresis loop is common in relaxor ferroelectrics even in normal ferroelectrics [42,43]. Obviously, the double P–E loop should not be considered as decisive evidence for the existence of antiferroelectrics. Recently, some researchers have realized that the appearance of the constricted hysteresis loop in BNT-based ceramics is due to an ergodic relaxor to a long-range ferroelectric phase transition [44]. They hold an opinion that the occurring of depolarization in BNT-based ceramics is due to the phase transition from long-range ferroelectric order to the relaxor state upon heating [44], not a structure phase transition from a low symmetry to a higher symmetry [45]. In the present study, the enhanced cation disorder in A-site and the decrease in spontaneous polarization, caused by the decrement of the B-site and O-site deviated distance from the locations of central symmetry cubic phase, destroy the long-range ferroelectric phase, thus T_d of the ceramics decreases with the increment of the La content.

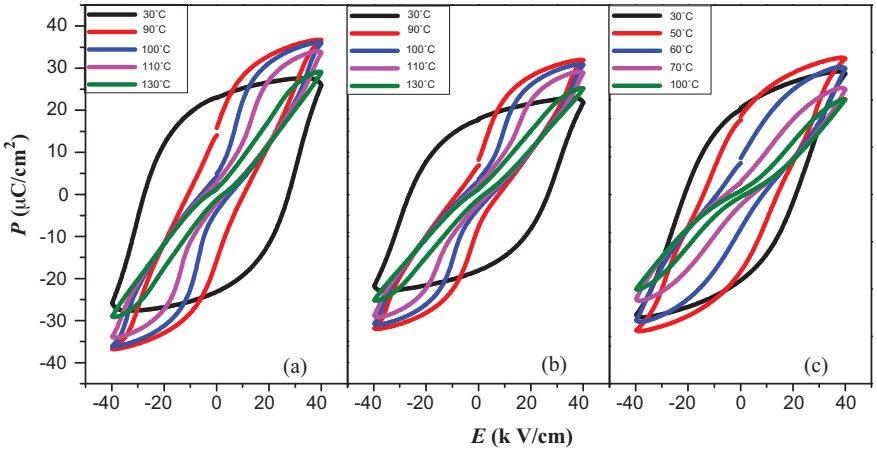

Fig. 8. P–E hysteresis loops of the $(Bi_{1-x}Na_{0.8}K_{0.2}La_x)_{0.5}TiO_3$ ceramics at different temperature: (a) $x = 0$, (b) $x = 0.005$, and (c) $x = 0.04$.

4. Conclusions

$(Bi_{1-x}Na_{0.8}K_{0.2}La_x)_{0.5}TiO_3$ lead-free piezoelectric ceramics have been prepared by conventional solid state sintering method. The XRD results reveal that La^{3+} has diffused into BNKT lattices to form a new solid solution of $(Bi_{1-x}Na_{0.8}K_{0.2}La_x)_{0.5}TiO_3$. Moderate substitution of La^{3+} for Bi^{3+} in the BNKT ceramics can enhance the piezoelectric properties of $(Bi_{1-x}Na_{0.8}K_{0.2}La_x)_{0.5}TiO_3$ ceramics. $(Bi_{0.995}Na_{0.8}K_{0.2}La_{0.005})_{0.5}TiO_3$ ceramic has the highest piezoelectric performance and strong ferroelectricity: piezoelectric coefficient $d_{33} = 155$ pC/N; electromechanical coupling factors $k_p = 29.5\%$ and $k_t = 47.3\%$; mechanical quality factor $Q_m = 110$; remnant polarization $P_r = 20.2\ \mu C/cm^2$; coercive field $E_c = 27.2$ kV/cm. The piezoelectric and ferroelectric properties of $(Bi_{1-x}Na_{0.8}K_{0.2}La_x)_{0.5}TiO_3$ ceramics deteriorate at the high La^{3+} level ($x > 0.04$) and the depolarization temperature moves to lower temperature. The decrement of T_d of the ceramics with the increment of the La content is caused by the enhanced cation disorder in A-site and the declined spontaneous polarization caused by the decrement of the B-site and O-site deviated distance from the locations of central symmetry cubic phase. When $x = 0.02$, a maximum strain of 0.16% is achieved in the $(Bi_{1-x}Na_{0.8}K_{0.2}La_x)_{0.5}TiO_3$ ceramic.

Acknowledgments

This work was supported by the National Natural Science Foundation of China (51002082, 11004113), Natural Science Foundation of Zhejiang Province (Y4090057), Natural Science Foundation of Ningbo (2009A610016, 201201A6105044), the Outstanding (Postgraduate) Dissertation Growth Fundation of Ningbo University (PY20110011) and the K.C. Wong Magna Foundation in Ningbo University (XYL10012, xkz11203).

References

[1] B. Jaffe, W.R. Cook, H. Jaffe, Piezoelectric Ceramics, Academic, New York, 1971.
[2] Y. Satio, H. Takao, T. Tani, T. Nonoyama, K. Takatori, T. Homma, T. Nagaya, M. Nakamura, Nature 432 (2004) 84–87.
[3] A. Herabut, A. Safari, J. Am. Ceram. Soc. 80 (1997) 2954.
[4] F. Ni, L. Luo, X. Pan, Y. Zhang, H. Chen, J. Mater. Sci. (2011), doi:10.1007/s10853-011-6177-1.
[5] T. Takenaka, K. Maruyama, K. Sakata, Jpn. J. Appl. Phys. 30 (1991) 2236–2239.
[6] T. Zhou, R. Huang, X. Shange, F. Peng, J. Guo, L. Chai, H. Gu, Y. He, Appl. Phys. Lett. 90 (2007) 182903.
[7] X.Y. Zhou, H.S. Gu, Y. Wang, W.Y. Li, T.S. Zhou, Mater. Lett. 59 (2005) 1649.
[8] M. Izumi, K. Yamamoto, M. Suzuki, Y. Noguchi, M. Miyayama, Appl. Phys. Lett. 93 (2008) 903.
[9] A. Sasaki, T. Chiba, Y. Mamiya, E. Otsuti, Jpn. J. Appl. Phys. 38 (1999) 5564–5567.
[10] D. Lin, K.W. Kwok, H.L.W. Chan, Solid State Ionics 178 (2008) 1930.
[11] C. Zhou, X. Liu, Mater. Chem. Phys. 108 (2008) 413.
[12] H. Ishii, H. Nagata, T. Takenaka, Jpn. J. Appl. Phys. 40 (2001) 5560.
[13] Q. Zheng, C. Xu, D. Lin, et al., J. Phys. D: Appl. Phys. 41 (2008) 125411.
[14] T. Zhou, R. Huang, X. Shang, et al., Appl. Phys. Lett. 90 (2007) 182903.
[15] X. Zhou, H. Gu, Y. Wang, et al., Mater. Lett. 59 (2005) 1649.
[16] G.O. Jones, P.A. Thomas, Acta Crystallogr. B 58 (2002) 168–178.
[17] S. Gorfman, P.A. Thomas, J. Appl. Crystallogr. 43 (2010) 1409–1414.
[18] E. Aksel, J.S. Forrester, J.L. Jones, et al., Appl. Phys. Lett. 98 (2011) 152901.
[19] W. Jo, J. Rödel, et al., Appl. Phys. Lett. 99 (2011) 042901.
[20] J.E. Daniels, W. Jo, J. Rödel, J.L. Jones, Appl. Phys. Lett. 95 (2009) 032904.
[21] K.T.P. Seifert, W. Jo, J. Rödel, J. Am. Ceram. Soc. 93 (2010) 1392–1396.
[22] R. Ranjan, A. Dviwedi, Solid State Commun. 135 (2005) 394–399.
[23] W. Jo, J.E. Daniels, J.L. Jones, X. Tan, P. Thomas, D. Damjanovic, J. Rödel, J. Appl. Phys. 109 (2011) 014110.
[24] Y.Q. Yao, T.Y. Tseng, C.C. Chou, H.H.D. Chen, J. Appl. Phys. 102 (2007) 094102.
[25] Y.S. Sung, J.M. Kim, J.H. Cho, T.K. Song, M.H. Kim, H.H. Chong, T.G. Park, D. Do, S.S. Kim, Appl. Phys. Lett. 96 (2010) 022901.
[26] Y. Hiruma, H. Nagata, T. Takenaka, J. Appl. Phys. 105 (2009) 084112.
[27] Y. Hiruma, H. Nagata, T. Takenaka, J. Appl. Phys. 104 (2008) 124106.
[28] C.R. Zhou, X.Y. Liu, W.Z. Li, C.L. Yuan, Solid State Commun. 149 (2009) 481.
[29] C. Xu, D. Lin, K.W. Kwok, Solid State Sci. 10 (2008) 934–940.
[30] G. Fan, W. Lu, X. Wang, F. Liang, J. Xiao, J. Phys. D: Appl. Phys. 41 (2008) 035403.
[31] H. Ni, L. Luo, W. Li, Y. Zhu, H. Luo, J. Alloys Compd. 509 (2011) 3958.
[32] K. Yoshii, Y. Hiruma, H. Nagata, T. Takenaka, Jpn. J. Appl. Phys. 45 (2006) 4493.
[33] Q. Xu, D. Huang, M. Chen, W. Chen, H. Liu, B. Kim, J. Alloys Compd. 471 (2008) 310.
[34] Y. Guo, M. Gu, H. Luo, Y. Liu, R. Withers, Phys. Rev. B 83 (2011) 054118.
[35] Y. Guo, M. Gu, H. Luo, J. Am. Ceram. Soc. 94 (2011) 1350–1353.
[36] J. Suchanicz, J. Kusz, H. Böhm, H. Duda, J.P. Mercurio, J. Eur. Ceram. Soc. 22 (2003) 1559.
[37] J. Suchanicz, J. Kusz, H. Böhm, Mater. Sci. Eng. B 97 (2003) 154.
[38] S. Zhang, A.B. Kounga, E. Aulbach, H. Ehrenberg, J. Rödel, Appl. Phys. Lett. 91 (2007) 112906.
[39] L. Wu, D. Xiao, F. Zhou, Y. Teng, Y. Li, J. Alloys Compd. 509 (2011) 466.
[40] Y. Dai, S. Zhang, T. Shrout, X. Zhang, J. Am. Ceram. Soc. 93 (2010) 1108–1113.
[41] S. Zhang, A.B. Kounga, W. Jo, C. Jamin, K. Seifert, T. Granzow, J. Rödel, D. Damjanovic, Adv. Mater. 21 (2009) 4716–4720.
[42] X. Ren, Nat. Mater. 3 (2004) 91.
[43] Z. Feng, X. Ren, Phys. Rev. B 77 (2008) 134115.
[44] W. Jo, S. Schaab, E. Sapper, L.A. Schmitt, H. Kleebe, et al., J. Appl. Phys. 110 (2011) 074106.
[45] E. Aksel, J.S. Forrester, B. Kowalski, et al., Appl. Phys. Lett. 99 (2011) 222901.